Coral Reefs
https://doi.org/10.1007/s00338-023-02417-0

REPORT

Porites astreoides coral populations demonstrate high clonality and connectivity in southeast Florida

Erin N. Shilling[1] · **Ryan J. Eckert**[1] · **Alexis B. Sturm**[1] · **Joshua D. Voss**[1]

Received: 24 August 2022 / Accepted: 21 August 2023

Abstract Coral reefs in southeast Florida have experienced severe losses in coral cover and diversity in recent decades, primarily due to disease outbreaks and bleaching events exacerbated by anthropogenic impacts. Subsequent increases in "weedy" coral species like *Agaricia* spp. and *Porites* spp. have been observed on many reefs in this region. At the northernmost boundary of the Florida's Coral Reef, St. Lucie Reef in Martin County has experienced a particularly notable increase in the abundance of *Porites astreoides*. To identify potential larval sources and *P. astreoides* population dynamics that may be contributing to observed coral community shifts, we sampled *P. astreoides* across five locations in southeast Florida from St. Lucie Reef to Fort Lauderdale and assessed population genetic structure using 2bRAD sequencing to generate single-nucleotide polymorphism (SNP) data. We identified high rates of clonality within and among the sample populations. Despite the brooding reproductive strategy of *P. astreoides*, there were relatively high levels of connectivity among populations and varying levels of genetic structure which correlated with geographic gradients. The genetic diversity and connectivity data reported here for *P. astreoides* populations in southeast Florida suggest that recent increases in abundance may be driven by high fecundity and long-range dispersal of a few successful genotypes.

Keywords Population genetics · *Porites astreoides* · Southeast Florida · Genetic connectivity · Single-nucleotide polymorphisms · 2bRAD

Introduction

Losses of large, primary reef-building corals in Florida and the wider Caribbean have been well documented over several decades (Gardner et al. 2003; Alves et al. 2022) and linked to both natural and anthropogenic stressors including global warming (Baker et al. 2008; Frölicher et al. 2018), hurricanes (Gardner et al. 2005; Dahlgren et al. 2020), ocean acidification, and nutrient pollution (Aronson and Precht 2001; Carpenter et al. 2008; IPCC 2014; Jackson et al. 2014). These stressors also correspond with increased incidence and intensity of bleaching events and disease outbreaks, both of which can lead to significant declines in coral cover (Sutherland et al. 2004; Harvell et al. 2007; Ruiz-Moreno et al. 2012; Vega Thurber et al. 2014; Tracy et al. 2019). The most recent severe coral disease outbreak, stony coral tissue loss disease (SCTLD), has contributed even further to the decline of coral cover and diversity on reefs in Florida and the wider Caribbean (Precht et al. 2016; Walton et al. 2018; Alvarez-Filip et al. 2019; Estrada-Saldívar et al. 2020; Brandt et al. 2021; Costa et al. 2021; Dahlgren et al. 2021). Since SCTLD was first documented near Miami, Florida in 2014, it has spread along the entirety of Florida's Coral Reef (Precht et al. 2016; Walton et al. 2018).

Throughout the Caribbean these disturbance events and subsequent losses of dominant coral cover have been followed by a proliferation of "weedy" stony coral species

Supplementary Information The online version contains supplementary material available at https://doi.org/10.1007/s00338-023-02417-0.

✉ Erin N. Shilling
eshilling15@gmail.com

Joshua D. Voss
jvoss2@fau.edu

[1] Harbor Branch Oceanographic Institute, Florida Atlantic University, Fort Pierce, FL, USA

Published online: 04 September 2023

including *Agaricia* spp., *Siderastrea* spp., and *Porites* spp. (Green et al. 2008; Walton et al. 2018; Jones et al. 2020; Eagleson et al. 2021; Heres et al. 2021). The Southeast Florida Coral Reef Evaluation and Monitoring Project (SECREMP) has reported increases in *P. astreoides, P. porites*, and *Agaricia* spp. colony abundance from 2013 to 2020 (Walton et al. 2018; Hayes et al. 2022). In 2019, *P. astreoides* was the most common coral species documented across all SECREMP sites, with *P. astreoides*, *Agaricia* spp., and *Siderastrea* spp. also comprising the majority of all coral recruits and juveniles < 4 cm in diameter (Gilliam et al. 2020). The replacement of larger, hermatypic coral colonies like Orbicellids and *Montastraea cavernosa* by these weedy species with less rugose morphologies represent a potential decrease in habitat structural complexity, as well as overall rates of carbonate accretion, which characterize and support the biodiversity of coral reefs (Alvarez-Filip et al. 2013; Graham and Nash 2013; Perry et al. 2015; Kuffner and Toth 2016). It has been argued that this change in community structure represents a significant ecological shift that is unmatched in the geologic record (Toth et al. 2019).

The observed recent increases in *P. astreoides* abundance and cover in southeast Florida are likely linked in part to the species' relatively low susceptibility to SCTLD as well as its reproductive strategies (NOAA 2018). *Porites astreoides* is a brooding coral species that holds its fertilized, developing embryos within its polyps and releases relatively large planula larvae that mature quickly (Chornesky and Peters 1987; Soong 1991). Additionally, *P. astreoides* spawn multiple times each year and have been shown to both self-fertilize and undergo internal fertilization after receiving gametes from other colonies (Szmant 1986; Brazeau et al. 1998). One ex situ experiment even showed the potential for *P. astreoides* colonies to reproduce parthenogenetically, a process where an unfertilized egg is able to develop into an embryo (Vollmer 2018). Therefore, it is possible that many of the new colonies observed on St. Lucie Reef and other reefs in the region are clones or at least very closely related to each other, depending also upon the level of gene flow among *P. astreoides* populations.

In addition to apparent resistance to disease and high fecundity, *P. astreoides* has been considered a hardy species for decades, as some populations have displayed significant heat tolerance (Kenkel et al. 2013), and the species is present across a wide range of depths (Engel and Bak 1979). These observations combined with documented increases in *P. astreoides* coverage led some to propose this species as an ecological "winner" in relatively degraded Caribbean reefs, a claim that had been relatively accepted (Green et al. 2008; Eagleson et al. 2021). However, the relative long-term success of this species under changing reef conditions is unknown, with at least one report suggesting a decline of this success under continued degradation of Caribbean reefs (Edmunds et al. 2021).

The primary aims of this study were to better understand the population genetic structure of *P. astreoides* in southeast Florida and to investigate genetic similarities that could potentially identify the mechanisms underlying their recent increases in abundance. To these ends, we employed a 2bRAD method to identify single-nucleotide polymorphisms (SNPs) and assess relative levels of connectivity, genetic structure, and clonality among *P. astreoides* populations at five sites across Martin, Palm Beach, and Broward counties in southeast Florida. Quantifying the genetic diversity and connectivity of *P. astreoides* may help to predict the resilience of these populations to ongoing and future stress events. This is crucial given that *P. astreoides* is now dominant across southeast Florida reefs and has recently increased in abundance on several reefs throughout the wider Caribbean (Green et al. 2008; Walton et al. 2018; Jones et al. 2020; Eagleson et al. 2021; Heres et al. 2021).

Materials and methods

Sample sites and collection

Porites astreoides samples were collected by SCUBA divers from January to March 2021 on five nearshore reef sites that were near but not within SECREMP monitoring stations in the southeast Florida region (Table 1, Fig. 1). In total, ninety

Table 1 Samples collected by population, with county, total samples collected (n_c), total samples sequenced successfully (n_s), number of unique multilocus genotypes retained after the removal of clones (n_g), percentage of the population that was comprised of clones, average collection depth in meters, and latitude and longitude of collection site

Population	County	n_c	n_s	n_g	*clonality*	Avg. depth (m)	Latitude	Longitude
St. Lucie Reef	Martin	30	30	3	90%	3.0	27.131667	−80.134033
Jupiter	Palm Beach	15	15	10	33%	21.7	26.897735	−80.016383
West Palm Beach	Palm Beach	15	13	7	46%	14.7	26.652387	−80.020682
Boynton Beach	Palm Beach	15	14	10	40%	18.9	26.523552	−80.031692
Ft. Lauderdale	Broward	15	15	6	60%	7.1	26.147580	−80.096100

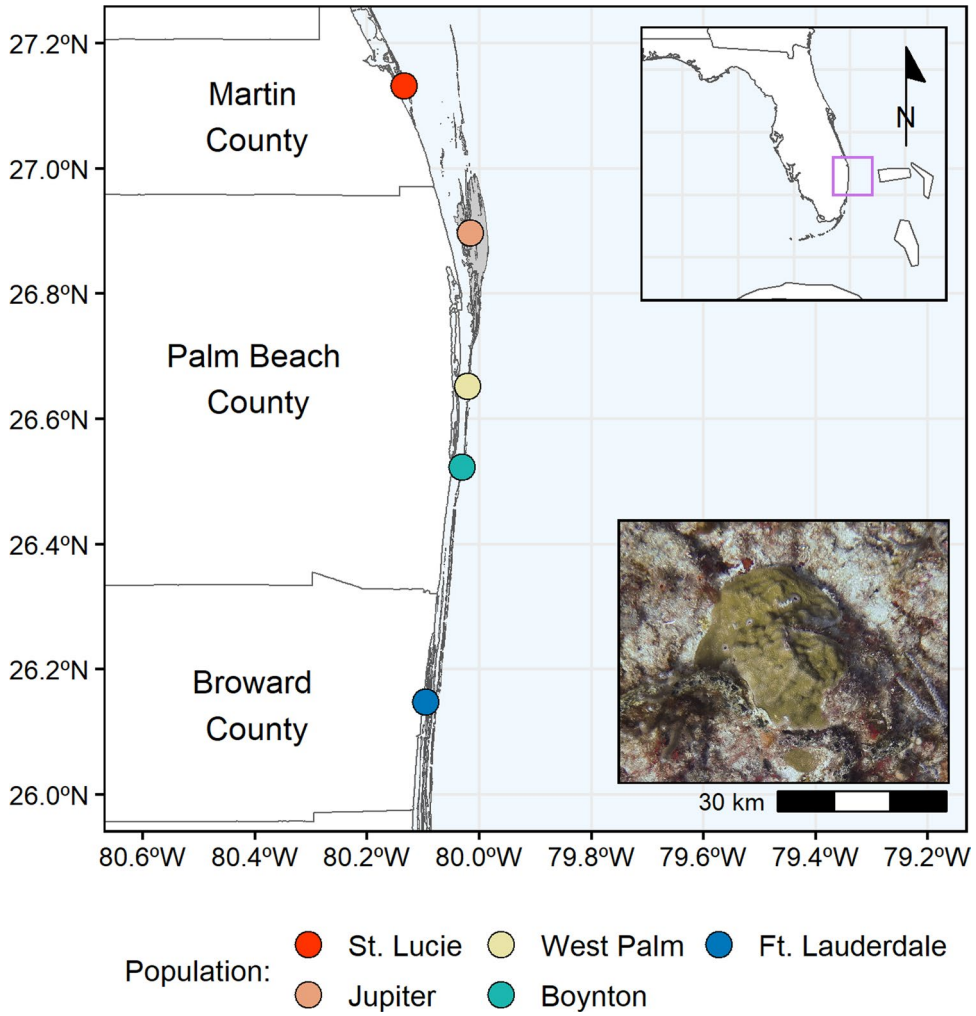

Fig. 1 Map of southeastern Florida coastline and hardbottom reef substrate coverage (light gray) with *Porites astreoides* sampling sites denoted with dots colored by population. Bottom right photograph shows a *P. astreoides* colony in situ

P. astreoides colonies were sampled, with approximately 2–5 cm^2 of tissue collected from each colony using a hammer and chisel. Sampled colonies were located at least 1 m from each other to decrease likelihood of sampling clones, but to still sample the dense population of St. Lucie Reef across a relatively fine spatial scale. Tissue samples were preserved in TRIzol in the field and put on ice during transport (4–6 h) to Harbor Branch Oceanographic Institute where they were stored at −80 °C until DNA extraction. Additionally, as there are two known color morphs of *P. astreoides*, brown and green/yellow (Gleason 1993), color was documented from photographs that were taken of each colony.

SNP library preparation

DNA was extracted from all samples using a modified dispersion buffer/phenol–chloroform–isoamyl alcohol extraction method (Sturm et al. 2020). DNA extracts were cleaned using the Zymo DNA Clean & Concentrator-5 kit and verified for sufficient quality and quantity. Library preparation followed a modified 2bRAD protocol based on Wang et al. (2012; https://github.com/z0on/2bRAD_denovo). Briefly, samples were digested using the type IIB restriction enzyme BcgI, then ligated to indexed adaptors for pooling. Three samples (termed "technical replicates") had libraries prepared in triplicate to allow for identification of clones during analysis (Manzello et al. 2019). Prior to pooling, successful digestion and ligation of all samples was verified via qPCR. Once verified, samples were pooled and eight pools of 12 samples were amplified using uniquely indexed Illumina sequencing adaptors, yielding unique, triple-indexed samples for sequencing. Amplification of the target band of ~ 180 bp was confirmed via gel electrophoresis, and equal volumes of the amplicons were pooled, concentrated, and quantified prior to sequencing. The final pool of 96 samples was sent to UT Austin's Genomic Sequencing and Analysis Facility, where automated size selection with Pippin Prep was completed

before sequencing on an Illumina NovaSeq with an SP flowcell using SR100 chemistry.

Genotyping and clonality

Sequence reads were demultiplexed and trimmed using custom Perl scripts (https://github.com/z0on/2bRAD_denovo). Sequences were then quality filtered using *cutadapt* v1.18, removing reads with a Phred quality score < 15 (Martin 2011). High-quality reads were mapped using the Bowtie2 aligner to a concatenated Symbiodiniaceae metagenome from the currently available *Symbiodinium microadriaticum* (Aranda et al. 2016), *Breviolum minutum* (Shoguchi et al. 2013), *Cladocopium goreaui* (Liu et al. 2018), and *Durusdinium trenchii* (Shoguchi et al. 2021) genomes. All sequences that did not align to the Symbiodiniaceae reference were then aligned to the *P. astreoides* genome using Bowtie2 (Langmead and Salzberg 2012; Wong and Putnam 2022).

All figures were generated in the *R* statistical environment v4.1.1; the code and data to generate figures and run statistical analyses are publicly available (https://github.com/erin-shilling/SEFL_Pastreoides_2bRAD). *ANGSD* was used to calculate genotype likelihoods with the filters: Minimum mapping quality scores of 20, maximum depth of 10 × the number of individuals, and loci were only retained if they were present in at least 50% of the individual samples; and then to create an identity-by-state (IBS) matrix for all samples with the following filters: minimum mapping quality scores of 20, minimum base quality scores of 30, minimum *p*-value for deviation from Hardy–Weinberg equilibrium of 10^{-5}, minimum p-value for strand bias of 10^{-5}, the removal of any tri-allelic SNPs, at least 70% of non-missing genotypes across samples, *p*-value of 10^{-6} that a locus is variable, and a minimum allele frequency of 0.05 (Korneliussen et al. 2014, https://github.com/z0on/2bRAD_denovo). A hierarchical cluster dendrogram was created from the IBS matrix and used to identify natural genetic clones by comparing them to the level of genetic similarity exhibited by the technical replicates included in the sample set. Based on which sample had the highest proportion of reads with at least 5X coverage, all but one of each clonal or technical replicate group were removed from the dataset. *ANGSD* was then rerun on the clones-removed dataset, using the same filters mentioned previously, to identify SNPs for subsequent analyses.

Coral population structure

An analysis of molecular variance (AMOVA, 999 permutations) was conducted using the program *poppr* v2.9.2 and *adegenet* v2.1.4 on the BCF file produced by *ANGSD* (Jombart et al. 2021). A distance-based redundancy analysis (dbRDA) was conducted on the IBS matrix to assess if environmental variables significantly explained any of the genetic variation observed (Kamvar et al. 2021). For the dbRDA, marine data layers were downloaded in *R* from BioOracle v2.2 using the package *sdmpredictors* v0.2.11 and present-day (long-term averages between 2000 and 2014) environmental parameters were extracted from the sites' geographic coordinates (Tyberghein et al. 2012; Assis et al. 2018; Bosch et al. 2022). Following methods implemented in Galaska et al. (2021), collinearity was assessed for all environmental variables. When two variables had a significant absolute correction coefficient ≥|0.7|, the most ecologically relevant variable was retained for subsequent analyses (Dormann et al. 2013). Additionally, the variance inflation factor (VIF) was calculated for the remaining variables and only variables with VIF < 10, the accepted threshold for preventing issues from multiple collinearities, were retained. Next, to account for population structure in the RDA, a PCA was run on the IBS matrix and the PCs which explained the majority of the variance were retained as explanatory variables in the RDA (Capblancq and Forester 2021). Then, using the function *ordiR2step* in *vegan* v2.5-7, a forward selection analysis of variance (ANOVA) was run to determine how much, if at all, each variable contributed to the amount of variance explained and to select the model that best explained the genetic variation (Oksanen et al. 2020). Subsequently, a principal coordinates analysis was run on those fitted values. Variance partitioning was assessed using *varpart* from the *vegan* package, and significance was assessed using ANOVAs (Oksanen et al. 2020).

Pairwise F_{ST} values for each population were calculated using *StAMPP* v1.6.3 package (Pembleton 2021). Population structure was assessed using *NGSadmix* for $K = 1 - 8$. (The number of populations sampled plus 3 to identify potentially cryptic clusters; Skotte et al. 2013.) The most likely value of *K* was estimated through both the Evanno method, implemented with the program CLUMPAK, and the Puechmaille method, implemented with the program StructureSelector (Kopelman et al. 2015; Puechmaille 2016; Li and Liu 2018).

Population connectivity

Estimated recent migration (two to three previous generations) of sample populations was calculated using BayesAss v3.04 with 20 million MCMC repetitions, 3 million burn-in with the migration, allele frequency, and inbreeding parameters set to 0.32, 0.80, and 0.0039, respectively, to reach targeted acceptance rates of 20–60% (Wilson and Rannala 2003; Mussmann et al. 2019). Visual assessment of convergence of runs was confirmed using Tracer v1.7.2, and deviance among model runs was analyzed in *R* (Rambaut et al. 2018). The trace file with the lowest Bayesian deviance was used to calculate migration

coefficients for each population acting as a source and sink, using the packages *TeachingDemos* and *LaplacesDemon* (Snow 2020; Hall et al. 2021). It should be noted that one of the population sample sizes used in this analysis, St. Lucie Reef, was lower than most recommendations for estimations of migration (Wilson and Rannala 2003; Meirmans 2014).

Genetic diversity and F_{ST} identified across most likely K

SNPs were filtered to only include those present in all the identified *K* genetic clusters after the *NGSadmix* population structure analysis was conducted. Individuals were considered to belong to a genetic lineage if they had > 75% likelihood to a putative lineage (Fifer et al. 2022). This was performed for both SNPs and all RAD loci (i.e., variant and invariant loci), using the sites flag in *ANGSD*. To compare genetic clustering by regional population vs. lineage, a dendrogram was generated in the same manner as described previously, but with samples colored by lineage.

Across these putative lineages, heterozygosity was calculated across all loci in *R* using *ANGSD* outputs (Korneliussen et al. 2014; https://github.com/z0on/2bRAD_denovo). Inbreeding coefficients for all samples were calculated using the software *NgsRelate* (Korneliussen and Moltke 2015). Differences in heterozygosity and inbreeding coefficients among lineages, as well as depth distribution (with clones re-included for only this depth analysis), were assessed using one-way ANOVAs. Tukey's tests were run as post hoc analysis for significant ANOVAs using the package *rstatix* v0.7.0 (Kassambara 2021). Pairwise F_{ST} values for each lineage were also calculated using the same methods described previously to compare to those calculated across regional populations.

Symbiodiniaceae classification

The number of sequences that aligned to each of the four Symbiodiniaceae genera in the metagenomic reference was counted for each individual, serving as a proxy of relative abundances for the four Symbiodiniaceae genera in each sample (Manzello et al. 2019). This analysis was conducted on both the clones-included and clones-removed datasets to examine if algal symbiont communities varied among clonal coral hosts.

Results

Genome alignment and clonality

Sequencing produced a total of 231 million raw reads before filtering, with an average of 2.4 million reads for each sample. After the removal of PCR duplicates, trimming, and quality filtering, 148 million reads remained with an average of 1.5 million reads per sample. Three unique samples failed to sequence, two from West Palm and one from Boynton (Table 1). The average alignment rate to the genome for all samples was 68.85%, with a range of 15.43–92.16%; the average alignment for samples that were retained for analysis (see below) was 86.55%, with a range of 66.89–92.16% (Supplemental Table 1). Three of the 90 individuals sampled were identified as the green/yellow color morph (one each at Jupiter, West Palm Beach, and St. Lucie). The low abundance of green/yellow colonies in SEFL limits any inferences relative to color that we could make with these data, and so this factor was not considered in subsequent analyses.

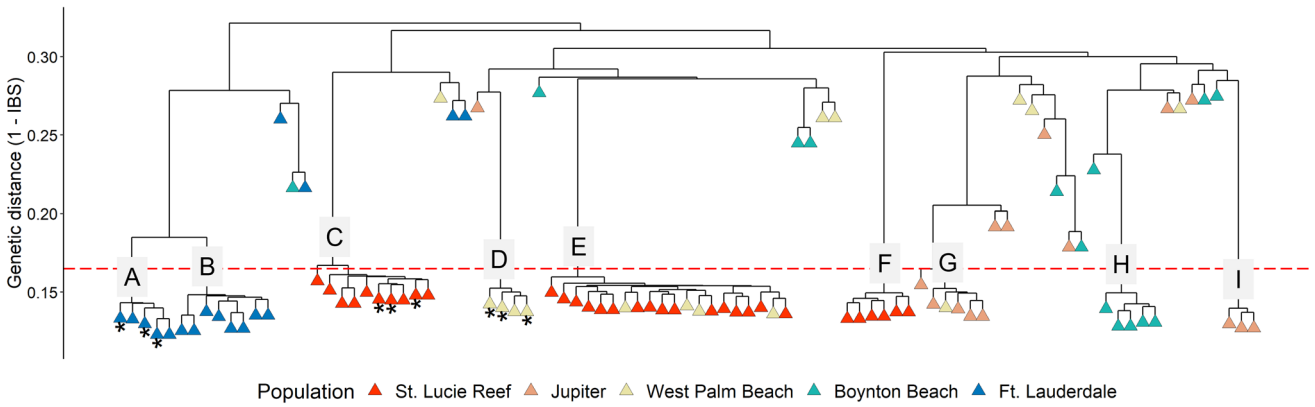

Fig. 2 Cluster dendrogram based on Identity-by-State matrix. Sample population is denoted by color, asterisks denote technical replicates. The dashed red line indicates the minimum genetic distance threshold for calling clonal individuals or groups and was determined by the lowest level at which the technical replicate groups were present. The nine clonal groups are labeled A–I directly above the corresponding cluster

From the cluster dendrogram, nine clonal groups were identified for a total of 51 naturally occurring clones (Table 1, Fig. 2). Each set of technical replicates were a part of one of these nine clonal groups. The overwhelming majority of the samples in each clonal group were from the same sampling site; however, two of the groups contained clones collected from different sites; group "E" included 16 samples from St. Lucie and four from West Palm, and group "G" included one sample from West Palm and four from Jupiter (Fig. 2). After the removal of all but one sample in each clonal group using methods described earlier, 36 unique individuals were retained for subsequent analyses (Table 1). The rate of clonality was highest at St. Lucie, with only three unique genotypes identified across the 30 samples, and lowest in Boynton, with 10 unique genotypes identified across the 14 samples (15 sampled, one failed to sequence) (Table 1, Fig. 2). After rerunning the clones and technical replicates-removed dataset in *ANGSD*, a total of 13,338 SNPs were identified.

Population structure

The AMOVA identified significant differences among the five sample populations, which explained 2.75% of the variation across samples (SS = 10,419.15, $p = 0.001$). The dbRDA indicated some overlap among Jupiter, West Palm, and Boynton sample populations while St. Lucie and Ft. Lauderdale were more distinct (Fig. 3). Three variables were retained for the model: depth, latitude, and nitrate, as well as the three PCs acting as a proxy for population evolutionary history. Nitrate (correlated with mean bottom light levels and chlorophyll levels) and the population structure PCs were removed as they were not selected for in the best model. The percent variation by depth (correlated with current velocity and mean bottom salinity) and latitude (correlated with cloud cover, dissolved oxygen, sea surface primary productivity, and sea surface temperature), respectively, is 5.09 and 4.81%, with a global variation of 9.06% (Table 2).

Significant pairwise differentiation between all populations except St. Lucie and West Palm was identified by the F_{ST} values (Fig. 4). Overall, Ft. Lauderdale had the highest F_{ST} values. Jupiter and Ft. Lauderdale populations were the most highly differentiated from each other ($F_{ST} = 0.070$).

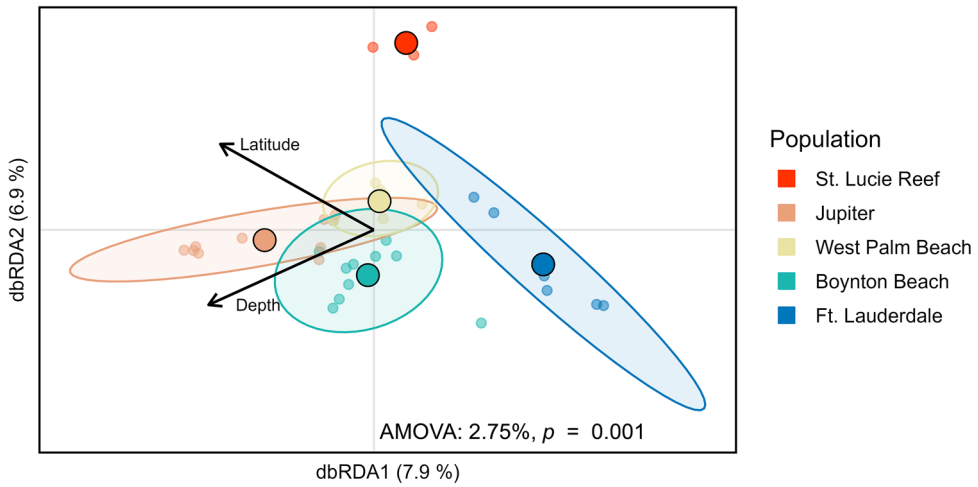

Fig. 3 Distance-based redundancy analysis results from Identity-by-State matrix showing clustering of samples by population, coded by color. Individual samples are represented by transparent circles while larger, solid circles represent the population centroids. Ellipses for each population (with the exception of the St. Lucie population due to low sample size) were calculated using multivariate t-distribution. The percent variation explained by population level differences calculated by the analysis of molecular variance is listed in the bottom right. Total variation explained by each axis is indicated. Vectors represent their corresponding environmental variables relative contribution to the variation displayed on the axes: latitude of sample collection and depth

Table 2 Environmental variables assessed in the dbRDA

Variable	Variance partition			ANOVA		
	Df	R^2	Adjusted R^2	SS	F	Pr(>F)
Depth	1	0.05092	0.02301	0.08212	1.8242	0.001
Latitude	1	0.04816	0.02017	0.07767	1.7204	0.001
All (global)	2	0.09061	0.03550	0.14613	1.6441	0.001

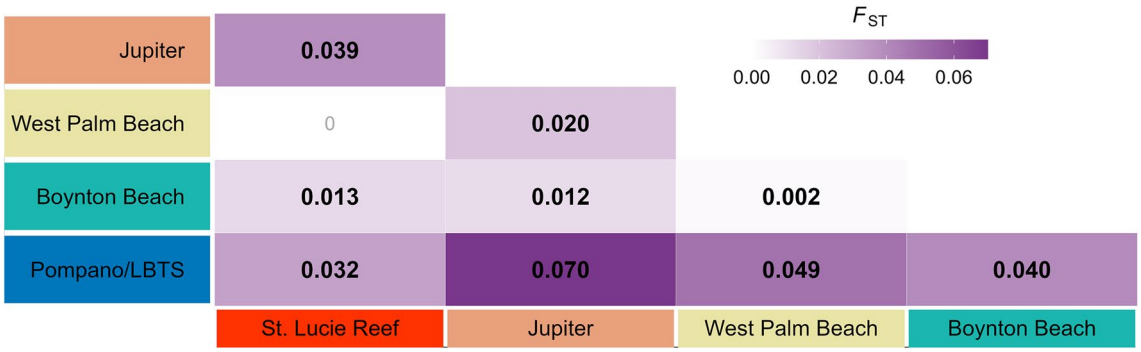

Fig. 4 Pairwise fixation index values (F_{ST}) for all populations sampled displayed as a heat map. Statistically significant values are bolded (post FDR-correction, $p < 0.05$)

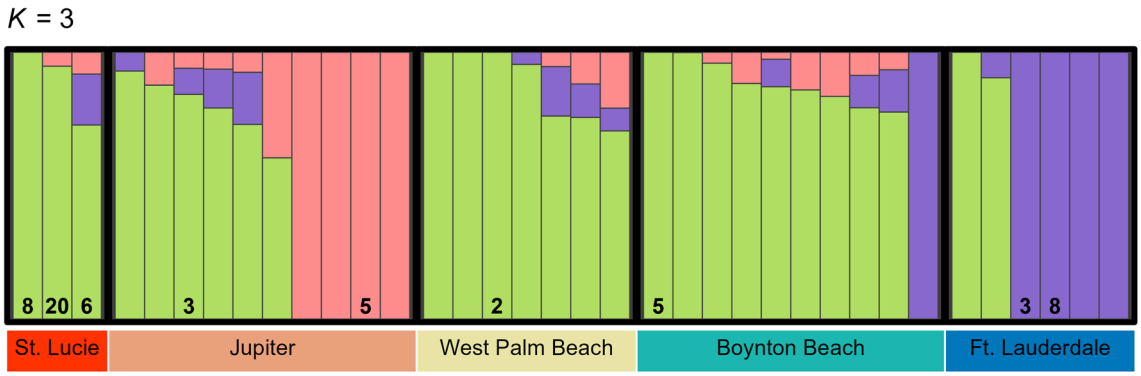

Fig. 5 StructureSelector's and CLUMPAK's calculated *K* showing three genetic lineages (represented by green, pink, and purple) of *Porites astreoides* present among the populations sampled. Each column represents one sample, and the proportion of each column filled with the color representing each lineage indicates the probability of membership to that lineage. Some individuals were from a clonal group, and the number of total individuals from that clonal group is represented by the numbers present at the base of the column; in some cases, this collapsed individuals from different sites into a column (see Fig. 2)

CLUMPAK analyses identified three as the optimal number of genetic lineages, while two of StructureSelector's reported *K* estimators selected $K = 2$, and the other two selected $K = 3$ (Fig. 5). After review of both *NGSadmix* plots, $K = 3$ was selected for subsequent interpretations and analyses given that it was the most frequently selected model. The first lineage (green) is relatively well distributed while the third (purple) is almost completely exclusive to Ft. Lauderdale. The northernmost site, St. Lucie, is dominated primarily by one lineage (green), and this same lineage was also predominant in the West Palm and Boynton populations. Jupiter is almost equally split in dominance by the first (green) and second lineage (pink), and the southernmost site in Ft. Lauderdale is primarily composed of the third (purple) lineage.

Genetic diversity and F_{ST} of lineages

Filtering to only retain SNPs present in all *K* genetic clusters resulted in 3228 SNPs. The cluster dendrogram colored by *K* showed clear clustering by the assigned *K*, with admixed individuals falling between or close to the intersection between lineages (Fig. 6). There was a significant difference in depth distributions across lineages, with the pink lineage comprised of significantly deeper samples than the green or purple lineages (Fig. 7a, one-way ANOVA, $F_{(2,75)} = 10.14$, $p < 0.001$; Tukey's test, both $p < 0.001$). It should be noted that depth was confounded with site in this study (Table 1). The green lineage had significantly higher levels of heterozygous RAD loci as compared to the purple and pink lineages (Fig. 7b, one-way ANOVA, $F_{(2,25)} = 11.4$, $p < 0.001$; Tukey's test, $p < 0.001$ and $p = 0.043$, respectively). None of the lineages had significantly different inbreeding coefficients from each other (Fig. 7c, one-way ANOVA, $F_{(2,29)} = 0.749$, $p = 0.482$). The F_{ST} between the green and purple lineages was highest at 0.065, followed by the pink and purple lineage F_{ST} of 0.053, and the lowest was between green and pink lineages at 0.044.

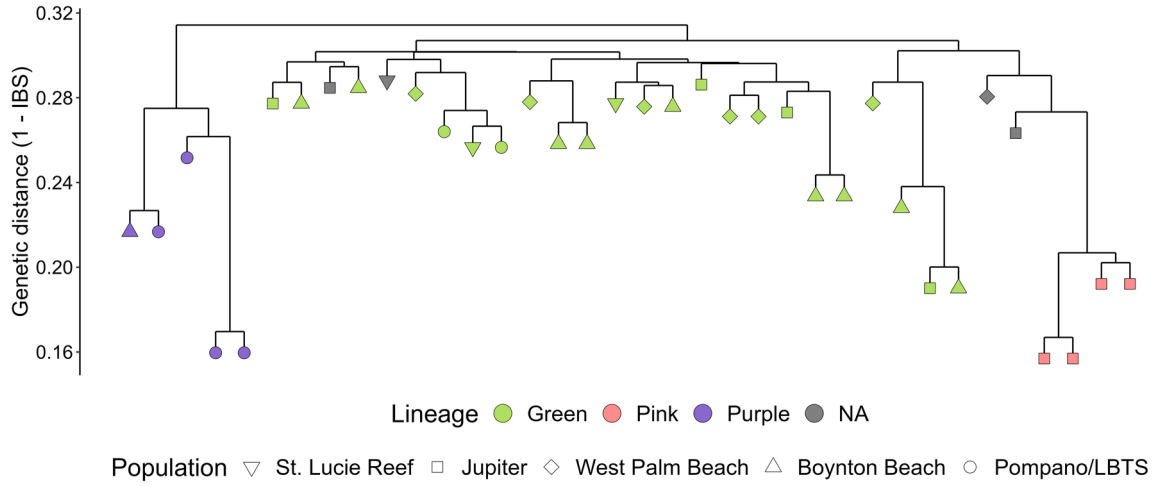

Fig. 6 Cluster dendrogram based on Identity-by-State matrix, with identified clones removed. Assigned lineage is denoted by color, sample population is denoted by shape

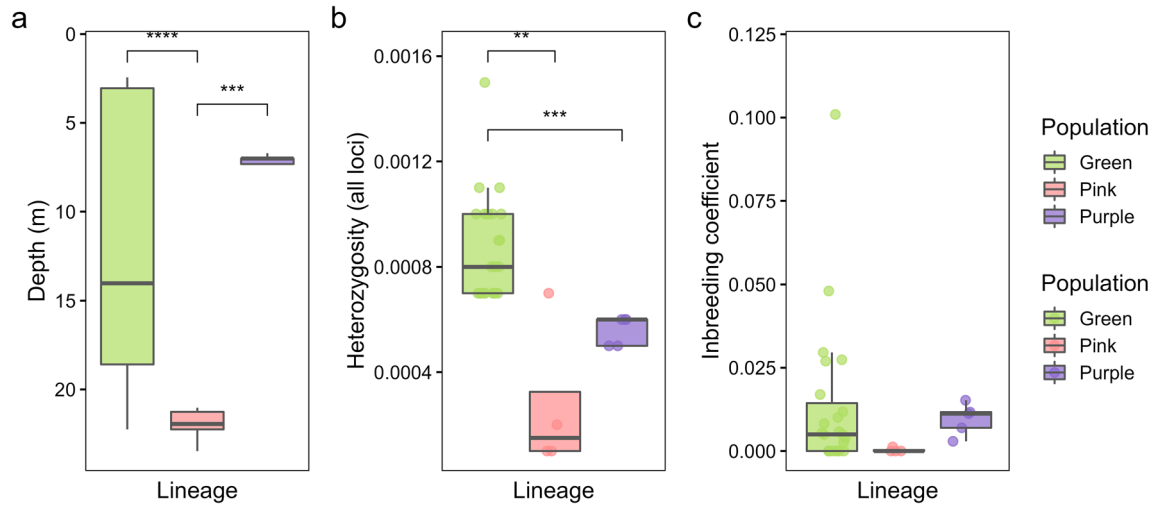

Fig. 7 Box and whisker plots displaying depth distribution, heterozygosity, and inbreeding across assigned lineages. a) depth of samples (with clones included) in each lineage, b) heterozygosity values calculated across all loci, c) inbreeding coefficients. Asterisks denote significant pairwise comparisons between lineages

Population connectivity

BayesAss analyses reported generally low rates of recent migration (*m*) ranging from 2.2 to 6.1% among St. Lucie, Jupiter, West Palm, and Ft. Lauderdale. However, Boynton was identified as a significant source population with migration rates estimated at 15.6–22.2% from Boynton to West Palm, Jupiter, and St. Lucie (Figs. 8 and 9).

Symbiodiniaceae communities

On average, 5.77% of the high-quality reads aligned to the Symbiodiniaceae metagenome. Of these, an average of 90% aligned to the *Symbiodinium* genus (Supplemental Fig. 1). On the clones removed dataset, three samples were dominated by *Cladocopium*, and all samples had at least some amount of *Symbiodinium*, *Breviolum*, *Cladocopium*, and *Durusdinium* present. In all but two instances, all clones in each clonal group identified had nearly identical symbiont assemblages (< 5% difference in abundance present in each genus). In the first instance, one sample collected in St. Lucie that is a part of clone group "E" contained 36% *Symbiodinium*, 48% *Cladocopium*, and 16% *Durusdinium*, while the 19 other samples (four from West Palm, 15 from St. Lucie) in that clonal group contained ~ 95% *Symbiodinium* (Fig. 2). In the second

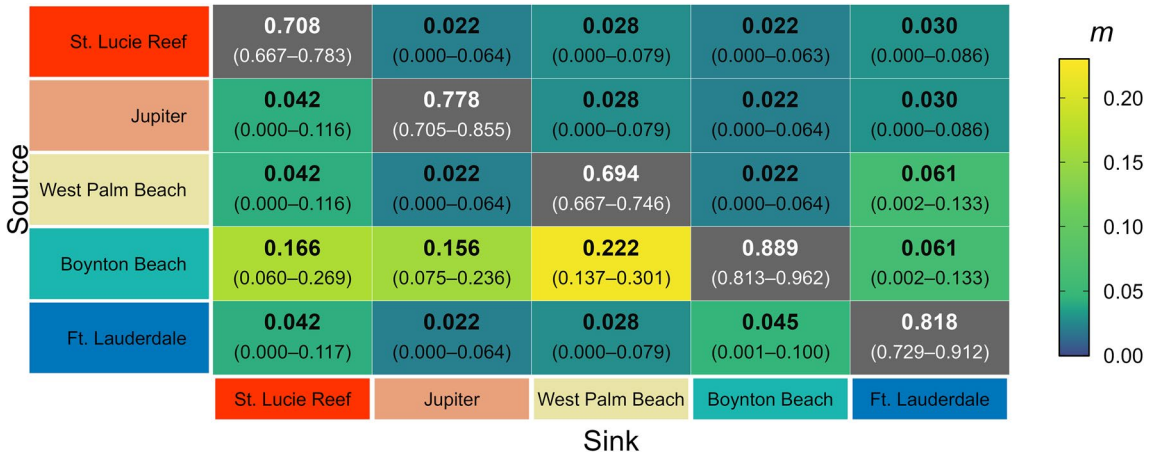

Fig. 8 Heat map of recent migration rates (*m*) inferred by BayesAss. Bolded numbers in each cell are estimates of *m* (mean of the posterior distribution) with uncertainty listed below (95% high posterior density [HPD] intervals). Gray cells indicate within-population retention rates

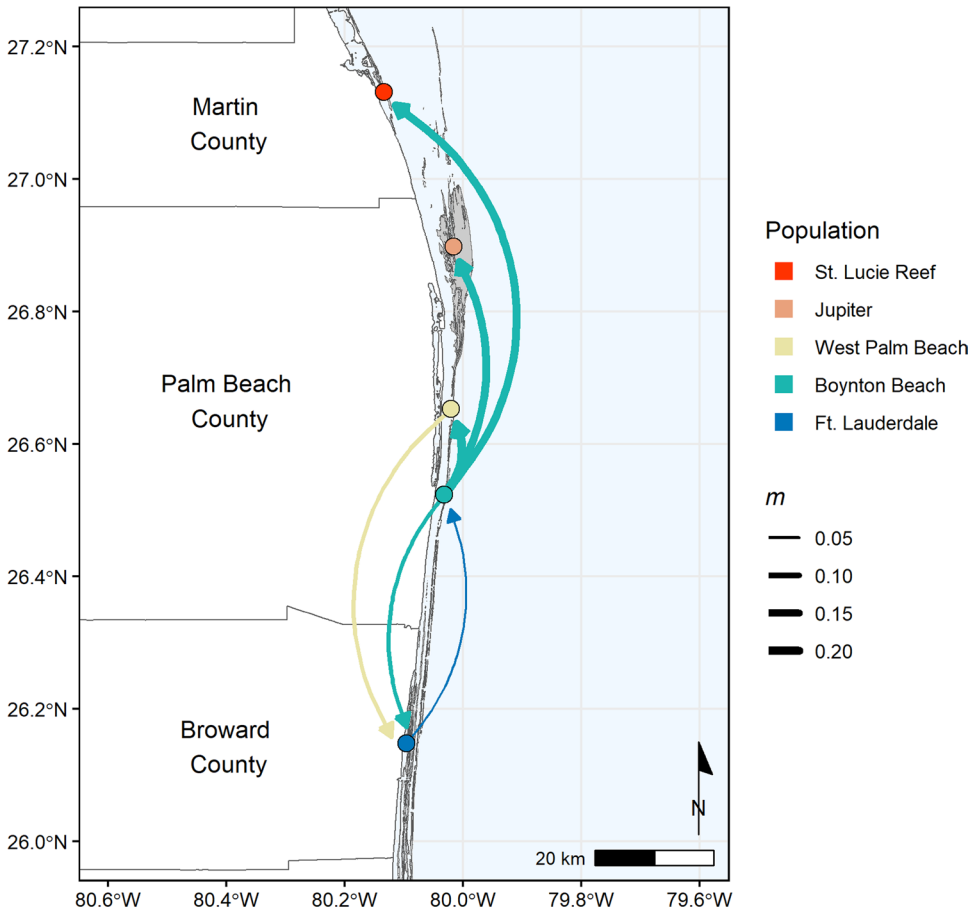

Fig. 9 Map of sample sites with arrows representing the levels of gene flow between populations. Circles are colored by population, as are arrows, indicating which population they originate from. Direction of arrows indicates the direction of gene flow, and width corresponds to the relative amount of gene flow. Only *m* values that had a > 0 lower 95% high posterior density [HPD] are displayed

instance, a sample collected from Jupiter that is a part of clonal group "I" contained a majority *Cladocopium* while the other two samples contained > 95% *Symbiodinium*.

It was also confirmed that there was no link between symbiont composition and color morph; all three of the previously mentioned yellow/green color morph individuals contained a majority (over 96%) *Symbiodinium*.

Discussion

This study found high rates of clonality of *P. astreoides* across all sites, with the highest proportional abundance of clones at St. Lucie (Table 1). Significant historical structuring of populations from St. Lucie to Ft. Lauderdale was observed as well and may be partially explained by associated variation in depth, latitude, and other spatial and environmental variables. However, there are also indications of relatively recent gene flow (over the past two–three generations), especially from Boynton to northern populations (Figs. 6, 7, 8). Symbiont communities were dominated by the genus *Symbiodinium*, which aligns with other studies of shallow (< 30 m) populations of *P. astreoides* (Thornhill et al. 2006; Kenkel et al. 2013; Serrano et al. 2016; Lenz et al. 2021). Overall, these data suggest that the relative success observed for *P. astreoides* in southeast Florida has been driven by the proliferation of a few genotypes which have become selected for under recent environmental conditions.

The average clonality rate found across sites in this study was 60%, which is high when compared to some other studies. However, in other comparable *P. astreoides* connectivity studies across the Caribbean, the rates of clonality measured seem to be correlated with the proximity of sampled colonies. Lower clonality rates around an average of 10% have been observed in studies which sampled colonies at distances of 5 m to 20 m apart from one another (Serrano et al. 2016; Gallery et al. 2021), while another study that sampled at roughly the same resolution as ours (at least 1 m, albeit with many of our samples collected farther apart than that) observed higher rates at 18% (Riquet et al. 2021). While exact distances among sampled colonies on a reef were not measured in this study, in the future these data may help identify how rates of clonality vary across different spatial scales.

Comparatively, a study on the branching *Porites divaricata* on an atoll in Belize identified an even higher rate of clonality, 92.6%, across 136 colonies over a ~ 500 m area (Lord et al. 2023). Like our study, they found that clones were primarily restricted to the same sub-sites sampled (within 100 m), however some were identified at distances of a few hundred meters apart. It should be noted that *P. divaricata* has been known to asexually reproduce through fragmentation (McDermond et al. 2014); however, due to their existence in a more protected mangrove habitat the authors proposed parthenogenesis to be more likely the main contributor to this pattern. While this sampling and analysis was more intensive across a smaller spatial scale than our study, it provides additional evidence that rates of asexual reproduction may be occurring more frequently than has previously been documented in Caribbean *Porites* species.

The high rates of clonality observed at our sites in southeast Florida have several implications, particularly at St. Lucie. First, it partially explains the recent rapid proliferation of *P. astreoides* colonies on St. Lucie. St. Lucie is likely not receiving a high influx of larvae from other populations recruiting to the reef, although there is evidence of connectivity with the Boynton population. High rates of self-fertilization by a few successful individuals, or increased asexual reproduction via fragmentation or parthenogenesis, may have occurred over recent years at St. Lucie. To further characterize the reproductive patterns driving the population dynamics and high rates of clonality at St. Lucie, histology could be utilized to quantify sex ratios and fecundity of colonies, as well as in situ larvae collection in combination with parentage analyses (Brazeau et al. 2005). Additionally, the observed high rate of clonality at St. Lucie forced a smaller usable sample set to assess connectivity for this study due to multiple analyses requiring the exclusion of clones to meet the necessary assumptions. Nonetheless, accurate conclusions can still be drawn from these results because ascertainment bias with low sample sizes (2–6) is not likely to be an issue so long as there is a high number of SNPs (i.e., in the thousands) which we were able to generate in this study (Willing et al. 2012; Nazareno et al. 2017). Finally, the presence of clones across adjacent sites (clonal groups were present across St. Lucie and West Palm [~ 80 km] as well as Jupiter and West Palm [~ 25 km]) is in themselves potential evidence that *P. astreoides* can disperse over several kilometers in this region. Whether this is occurring over a single generation through long-distance dispersal of parthenogenetically produced larvae, or over many generations through a stepping-stone method, remains to be understood.

This is the first study to assess the population genetics of *P. astreoides*, or any brooding stony coral, across the northern portion of Florida's Coral Reef. In the only other study of connectivity of a stony coral in the northern portion of Florida's Coral Reef, a broadcast spawning species, *Montastraea cavernosa,* was sampled across the same sites used in this study and were genotyped using microsatellites (Dodge et al. 2020). Both species exhibited high levels of differentiation between the Ft. Lauderdale populations and all other sites; however, for *P. astreoides* the Jupiter population was also highly differentiated (Fig. 3). Overall, populations of *P. astreoides* appear to have more genetic structure in this region than *M. cavernosa*, as might be expected for a brooder, and greater spatial differentiation than *P. astreoides* populations sampled on other Florida reefs (Serrano et al. 2016; Gallery et al. 2021).

While there is significant structuring across most sites, St. Lucie and West Palm populations were not differentiated, as indicated by the dbRDA, F_{ST} values, and admixture analyses (Figs. 3, 4, 5), suggesting that the St. Lucie *P. astreoides* population has historically been connected to the West

Palm population. Based on both migration modeling results and the lower F_{ST} values observed, Boynton appears to be a recent source population for all populations sampled north of it (Figs. 4, 8, and 9). This can possibly be explained by the general northward flow of the Florida Current. The green lineage exhibited significantly higher levels of heterozygosity, and the majority of genetically unique individuals in all populations belonged to this lineage, with the exception of Ft. Lauderdale.

The assumed northward flow of larvae from Boynton along the Florida Current does not adequately explain why the Ft. Lauderdale population is genetically isolated, as evidenced by its overall connectivity and structure results. The Ft. Lauderdale region lacks apparent physical barriers that would prevent northern or southern transport of larvae, and several modeling and population genetic studies provide evidence of larval dispersal and connectivity from Ft. Lauderdale to northern and southern reefs for other species (Baums et al. 2010; Bernard et al. 2019; Frys et al. 2020). It is possible that the relative isolation of this Ft. Lauderdale *P. astreoides* population is driven by its location on the inner reef bank, while all other sample sites were located on outer reef banks. Significant counter currents and eddies in this region have been characterized and may result in different directionality of larval transport on inner and outer reef banks (Fig. 1; Lee and Mayer 1977; Shay et al. 2002; Soloviev et al. 2003, 2017). Overall, it is difficult to make broad inferences about biophysical barriers in the northern portion of Florida's Coral Reef, since the majority of published studies of sessile, benthic species focus on connectivity south of Ft. Lauderdale and primarily on the Florida Keys, occasionally including sites in Palm Beach County (López-Legentil and Pawlik 2009; Baums et al. 2010; DeBiasse et al. 2016; Serrano et al. 2016; Drury et al. 2017; Bernard et al. 2019; Griffiths et al. 2020; Gallery et al. 2021; Rippe et al. 2021). In the Lower Florida Keys, Kenkel et al. (2013) found significant genetic divergence between inshore and offshore *P. astreoides* populations, thought to be driven by differences in thermotolerance of the genotypes. It is possible that some pre- or post-settlement barriers exist in Ft. Lauderdale such as thermal regimes, perhaps even some that are specific to coral larvae (*M. cavernosa* larvae showed significant differentiation at this site in the previously mentioned study, Dodge et al. 2020), which do not cause limitations for the dispersal of other marine benthic species for some reason. It is also possible that the genetic structuring of Ft. Lauderdale samples in this study would present differently in the context of a spatially larger dataset.

Regarding other *P. astreoides* populations assessed in Florida, Gallery et al. (2021) sampled *P. astreoides* in the Florida Keys and found evidence of panmixia throughout the Keys as well as high levels of gene flow, exhibiting overall stronger connectivity than we observed among *P. astreoides* populations in southeast Florida. Another study examined horizontal and vertical connectivity of *P. astreoides* populations across the Caribbean and found that shallow sites in the Florida Keys and the US Virgin Islands were highly connected to each other but differentiated from those in Bermuda (Serrano et al. 2016). Populations in Florida also exhibited significant depth-dependent genetic structuring similar to what we identified in this study; however, they were able to use a paired "shallow" (< 10 m) "deep" (> 25 m) design whereas we sampled distinct sites which differed by depth (3–22 m, Serrano et al. 2016). It should be noted that both of these studies utilized microsatellites markers as opposed to SNPs. Microsatellite markers have a reduced ability to identify fine-scale genetic differentiation among populations, when compared to large suites of SNP markers, and may have contributed to the higher localized levels of connectivity observed compared to this study (Sturm et al. 2020). Understanding dispersal and connectivity of species like *P. astreoides* is important as brooding coral species are becoming increasingly dominant on many Caribbean reefs. While brooding corals typically produce larvae that are competent to settle shortly after release and often have high levels of self-recruitment on reefs, brooders also have potential for long dispersal distances (Carlon and Olson 1993; Jones et al. 2009). In addition to the reports of panmixia for *P. astreoides* discussed above, *Siderastrea radians* populations in Brazil showed little genetic structuring over a range of more than 1600 km (Neves et al. 2008). Likewise, studies of *A. agaricites* across the Flower Garden Banks and the Caribbean (Brazeau et al. 2005) found similar results to Neves et al. (2008), as did a larger scale study of multiple brooding and spawning species along the Great Barrier Reef (Ayre and Hughes 2000), and a small-scale study in Puerto Rico on *A. lamarcki* (Hammerman et al. 2018). A connectivity study of *Favia fragum* identified significant differentiation across reefs in Barbados, Jamaica, Panama, and Bermuda, but relatively high levels of gene flow within the reefs sampled, further supporting the idea that the dispersal of brooded larvae does tend to be more limited than broadcast spawners, but can have localized high levels of connectivity (Goodbody-Gringley et al. 2010).

Overall, our results indicate that it is possible that a combination of sufficient genetic diversity provided by historic populations and the life history traits that support *P. astreoides* ability to relatively rapidly proliferate, including the production of clones, are aiding the species in filling reef niche space left by the mortality of other stony coral species (Estrada-Saldívar et al. 2019). The frequency of clones, and the apparent success of a few genotypes, could potentially foretell a short-lived "win" if low genetic diversity impacts population resilience. However, the reproductive and proliferation strategies of scleractinian corals are diverse and still not fully understood

(Hughes and Jackson 1980; Dubinsky and Stambler 2011), and through newly described mechanisms such as heritable somatic mutations (Vasquez Kuntz et al. 2022), communities may be able to maintain diversity and persist from populations which would not typically be considered viable for other species or in other environments.

To better understand connectivity and population persistence of *P. astreoides* and other brooding coral species with similar life histories on Caribbean reefs, further investigation using both high resolution population genetics and larval dispersal models is needed. As these species continue to emerge as apparent ecological "winners" in this region, the factors that may be driving their dispersal and success may be informative for regional scale approaches to coral management and restoration. Additionally, a better understanding of what biophysical factors influence larval dispersal of these corals on the northern portion of Florida's Coral Reef are important, as these often-overlooked reefs may be crucial sources of larvae and genetic diversity, both locally and for other regions across the Caribbean.

Acknowledgements We thank A. Klein, G. Pantoni, and A. Carreiro for assistance with sample collection and processing; J. Nelson and M. Roy for assistance with boating and diving operations; K. Kerrigan for feedback on experimental design; and the University of Texas at Austin's Genome Sequencing and Analysis Facility for sequencing support. Funding for this research was awarded to J. Voss from the Florida Department of Environmental Protection (B9657D and B7C241). All work was carried out under permission of Florida Fish and Wildlife Conservation Commission (permit SAL-20-1702-SRP) and St. Lucie Inlet State Park (permit #01221915). This is contribution 2317 from Harbor Branch Oceanographic Institute at Florida Atlantic University.

Author's contribution JDV conceived the study and secured the funding. ENS, JDV, and RJE developed the study design. ENS and RJE collected samples, ENS and ABS conducted the lab work. ENS, RJE, and ABS conducted the data analyses and visualizations. ENS wrote the manuscript, and all authors edited and contributed to the final version.

Data availability The sequence data for this study is available on NCBI under the following accession ID: PRJNA869314, https://www.ncbi.nlm.nih.gov/sra/PRJNA869314. All other data and code to conduct the analyses and generate the figures for this manuscript are available on GitHub: https://github.com/erin-shilling/SEFL_Pastreoides_2bRAD.

Declarations

Conflict of interest The authors declare no conflicts of interest.

References

Alvarez-Filip L, Carricart-Ganivet JP, Horta-Puga G, Iglesias-Prieto R (2013) Shifts in coral-assemblage composition do not ensure persistence of reef functionality. Sci Rep 3:1–5

Alvarez-Filip L, Estrada-Saldívar N, Pérez-Cervantes E, Molina-Hernández A, González-Barrios FJ (2019) A rapid spread of the stony coral tissue loss disease outbreak in the Mexican Caribbean. PeerJ 7:e8069

Alves C, Valdivia A, Aronson RB, Bood N, Castillo KD, Cox C, Fieseler C, Locklear Z, McField M, Mudge L, Umbanhowar J, Bruno JF (2022) Twenty years of change in benthic communities across the Belizean Barrier Reef. PLoS ONE 17:1–23

Aranda M, Li Y, Liew YJ, Baumgarten S, Simakov O, Wilson MC, Piel J, Ashoor H, Bougouffa S, Bajic VB, Ryu T, Ravasi T, Bayer T, Micklem G, Kim H, Bhak J, LaJeunesse TC, Voolstra CR (2016) Genomes of coral dinoflagellate symbionts highlight evolutionary adaptations conducive to a symbiotic lifestyle. Sci Rep 6:1–15

Aronson RB, Precht WF (2001) White-band disease and the changing face of Caribbean coral reefs. Hydrobiologia 460:25–38

Assis J, Tyberghein L, Bosch S, Verbruggen H, Serrão EA, De Clerck O (2018) Bio-ORACLE v2.0: Extending marine data layers for bioclimatic modelling. Glob Ecol Biogeogr 27:277–284

Ayre DJ, Hughes TP (2000) Genotypic diversity and gene flow in brooding and spawning corals along the Great Barrier Reef, Australia. Evolution (n y) 54:1590–1605

Baker AC, Glynn PW, Riegl B (2008) Climate change and coral reef bleaching: an ecological assessment of long-term impacts, recovery trends and future outlook. Estuar Coast Shelf Sci 80:435–471

Baums IB, Johnson ME, Devlin-Durante MK, Miller MW (2010) Host population genetic structure and zooxanthellae diversity of two reef-building coral species along the Florida Reef Tract and wider Caribbean. Coral Reefs 29:835–842

Bernard AM, Finnegan KA, Shivji MS (2019) Genetic connectivity dynamics of the giant barrel sponge, *Xestospongia muta*, across the Florida Reef Tract and Gulf of Mexico. Bull Mar Sci 95:161–175

Bosch S, Tyberghein L, De Clerck O, Fernandez S, Schepers L (2022) Package 'sdmpredictors', Species Distribution Modelling Predictor Datasets

Brandt ME, Ennis RS, Meiling SS, Townsend J, Cobleigh K, Glahn A, Quetel J, Brandtneris V, Henderson LM, Smith TB (2021) The emergence and initial impact of stony coral tissue loss disease (SCTLD) in the United States Virgin Islands. Front Mar Sci 8:1–15

Brazeau DA, Gleason DF, Morgan ME (1998) Self-fertilization in brooding hermaphroditic Caribbean corals: evidence from molecular markers. J Exp Mar Bio Ecol 231:225–238

Brazeau DA, Sammarco PW, Gleason DF (2005) A multi-locus genetic assignment technique to assess sources of *Agaricia agaricites* larvae on coral reefs. Mar Biol 147:1141–1148

Capblancq T, Forester BR (2021) Redundancy analysis: a Swiss Army Knife for landscape genomics. Methods Ecol Evol 12:2298–2309

Carlon DB, Olson RR (1993) Larval dispersal distance as an explanation for adult spatial pattern in two Caribbean reef corals. J Exp Mar Biol Ecol 173:247–263

Carpenter KE, Abrar M, Aeby G, Aronson RB, Banks S, Bruckner A, Chiriboga A, Cortes J, Delbeek JC, DeVantier L, Edgar GJ, Edwards AJ, Fenner D, Guzman HM, Hoeksema BW, Hodgson G, Johan O, Licuanan WY, Livingstone SR, Lovell ER, Moore JA, Obura DO, Ochavillo D, Polidoro BA, Precht WF, Quibilan MC, Reboton C, Richards ZT, Rogers AD, Sanciangco J, Sheppard A, Sheppard C, Smith J, Stuart S, Turak E, Veron JEN, Wallace C, Weil E, Wood E (2008) One-third of reef-building corals face elevated extinction risk from climate change and local impacts. Science (80-) 321:560–563

Chornesky EA, Peters EC (1987) Sexual reproduction and colony growth in the Scleractinian coral *Porites astreoides*. Biol Bull 172:161–177

Costa SV, Hibberts SJ, Olive DA, Budd KA, Long AE, Meiling SS, Miller MB, Vaughn KM, Carrión CI, Cohen MB, Savage AE, Souza MF, Buckley L, Grimes KW, Platenberg R, Smith TB, Blondeau J, Brandt ME (2021) Diversity and disease: the effects of coral diversity on prevalence and impacts of stony coral tissue loss disease in Saint Thomas, U.S. Virgin Islands Front Mar Sci 8:1–13

Dahlgren C, Pizarro V, Sherman K, Greene W, Oliver J (2021) Spatial and temporal patterns of stony coral tissue loss disease outbreaks in The Bahamas. Front Mar Sci 8:1–13

Dahlgren C, Sherman K, Haines L, Knowles L, Callwood K (2020) Bahamas Coral Reef Report Card Volume 2:2015–2020

DeBiasse MB, Richards VP, Shivji MS, Hellberg ME (2016) Shared phylogeographical breaks in a Caribbean coral reef sponge and its invertebrate commensals. J Biogeogr 43:2136–2146

Dodge DL, Studivan MS, Eckert RJ, Chei E, Beal J, Voss JD (2020) Population structure of the scleractinian coral *Montastraea cavernosa* in southeast Florida. Bull Mar Sci 96:767–782

Dormann CF, Elith J, Bacher S, Buchmann C, Carl G, Carré G, Marquéz JRG, Gruber B, Lafourcade B, Leitão PJ, Münkemüller T, Mcclean C, Osborne PE, Reineking B, Schröder B, Skidmore AK, Zurell D, Lautenbach S (2013) Collinearity: a review of methods to deal with it and a simulation study evaluating their performance. Ecography (cop) 36:27–46

Drury C, Schopmeyer S, Goergen E, Bartels E, Nedimyer K, Johnson M, Maxwell K, Galvan V, Manfrino C, Lirman D (2017) Genomic patterns in *Acropora cervicornis* show extensive population structure and variable genetic diversity. Ecol Evol 7:6188–6200

Dubinsky Z, Stambler N (2011) Coral reefs: an ecosystem in transition. Springer, Netherlands, Dordrecht

Eagleson RG, Lumsden JS, Álvarez-Filip L, Herbinger CM, Horricks RA (2021) Coverage increases of *Porites astreoides* in Grenada determined by shifts in size-frequency distribution. Diversity 13:1–15

Edmunds PJ, Didden C, Frank K (2021) Over three decades, a classic winner starts to lose in a Caribbean coral community. Ecosphere 12:1–14

Engel MS, Bak RPM (1979) Distribution, abundance and survival of juvenile hermatypic corals (Scleractinia) and the importance of life history strategies in the parent coral community. Mar Biol 54:341–352

Estrada-Saldívar N, Jordán-Dalhgren E, Rodríguez-Martínez RE, Perry C, Alvarez-Filip L (2019) Functional consequences of the long-term decline of reef-building corals in the Caribbean: evidence of across-reef functional convergence. R Soc Open Sci 6:1–15

Estrada-Saldívar N, Molina-Hernández A, Pérez-Cervantes E, Medellín-Maldonado F, González-Barrios FJ, Alvarez-Filip L (2020) Reef-scale impacts of the stony coral tissue loss disease outbreak. Coral Reefs 39:861–866

Fifer JE, Yasuda N, Yamakita T, Bove CB, Davies SW (2022) Genetic divergence and range expansion in a western North Pacific coral. Sci Total Environ 813:1–12

Frölicher TL, Fischer EM, Gruber N (2018) Marine heatwaves under global warming. Nature 560:360–364

Frys C, Saint-Amand A, Le Hénaff M, Figueiredo J, Kuba A, Walker B, Lambrechts J, Vallaeys V, Vincent D, Hanert E (2020) Fine-scale coral connectivity pathways in the Florida reef tract: implications for conservation and restoration. Front Mar Sci 7:1–16

Galaska MP, Liu G, West D, Erickson K, Quattrini AM, Bracco A, Herrera S (2021) Seascape genomics reveals metapopulation connectivity network of *Paramuricea biscaya* in the Northern Gulf of Mexico. Front Mar Sci 8:1–14

Gallery DN, Green ML, Kuffner IB, Lenz EA, Toth LT (2021) Genetic structure and diversity of the mustard hill coral *Porites astreoides* along the Florida Keys reef tract. Mar Biodivers 51:1–16

Gardner TA, Côté IM, Gill JA, Grant A, Watkinson AR (2003) Long-term region-wide declines in Caribbean corals. Science (80-) 301:958–960

Gardner TA, Côté IM, Gill JA, Grant A, Watkinson AR (2005) Hurricanes and Caribbean Coral Reefs: impacts, recovery patterns, and role in long-term decline. Ecology 86:174–184

Gilliam DS, Hayes NK, Ruzicka R, Colella M (2020) Southeast Florida coral reef evaluation and monitoring project; 2019 Year 17 Executive Summary

Gleason DF (1993) Differential effects of ultraviolet radiation on green and brown morphs of the Caribbean coral *Porites astreoides*. Limnol Oceanogr 38:1452–1463

Goodbody-Gringley G, Vollmer SV, Woollacott RM, Giribet G (2010) Limited gene flow in the brooding coral *Favia fragum (Esper, 1797)*. Mar Biol 157:2591–2602

Graham NAJ, Nash KL (2013) The importance of structural complexity in coral reef ecosystems. Coral Reefs 32:315–326

Green DH, Edmunds PJ, Carpenter RC (2008) Increasing relative abundance of *Porites astreoides* on Caribbean reefs mediated by an overall decline in coral cover. Mar Ecol Prog Ser 359:1–10

Griffiths SM, Taylor-Cox ED, Behringer DC, Butler MJ, Preziosi RF (2020) Using genetics to inform restoration and predict resilience in declining populations of a keystone marine sponge. Biodivers Conserv 29:1383–1410

Hall B, Hall M, Brown E, Hermanson R, Charpentier E, Heck D, Laurent S, Gronau QF, Singmann H (2021) Package 'LaplacesDemon': Complete Environment for Bayesian Inference

Hammerman NM, Rivera-Vicens RE, Galaska MP, Weil E, Appledoorn RS, Alfaro M, Schizas NV (2018) Population connectivity of the plating coral *Agaricia lamarcki* from southwest Puerto Rico. Coral Reefs 37:183–191

Harvell D, Jordán-Dahlgren E, Merkel S, Rosenberg E, Raymundo L, Smith G, Weil E, Willis B (2007) Coral disease, environmental drivers, and the balance between coral and microbial associates. Oceanography 20:172–195

Hayes NK, Walton CJ, Gilliam DS (2022) Tissue loss disease outbreak significantly alters the Southeast Florida stony coral assemblage. Front Mar Sci 9:1–18

Heres MM, Farmer BH, Elmer F, Hertler H (2021) Ecological consequences of Stony Coral Tissue Loss Disease in the Turks and Caicos Islands. Coral Reefs 40:609–624

Hughes TP, Jackson JBC (1980) Do corals lie about their age? Some demographic consequences of partial mortality, fission, and fusion. Science (80-) 209:713–715

IPCC (2014) Climate Change 2014 Synthesis Report. IPCC Fifth Assess Rep 151

Jackson J, Donovan M, Cramer K, Lam W (2014) Status and trends of Caribbean Coral Reefs 1970–2012

Jombart T, Kamvar ZN, Collins C, Lustrik R, Beugin M-P, Knaus BJ, Solymos P, Mikryukov V, Schliep K, Maié T, Morkovsky L, Ahmed I, Cori A, Calboli F, Ewing R, Michaud F, DeCamp R, Courtiol A (2021) Package 'adegenet', Exploratory Analysis of Genetic and Genomic Data

Jones GP, Almany GR, Russ GR, Sale PF, Steneck RS, Van Oppen MJH, Willis BL (2009) Larval retention and connectivity among populations of corals and reef fishes: history, advances and challenges. Coral Reefs 28:307–325

Jones NP, Figueiredo J, Gilliam DS (2020) Thermal stress-related spatiotemporal variations in high-latitude coral reef benthic communities. Coral Reefs 39:1661–1673

Kamvar ZN, Tabima JF, Everhart SE, Brooks JC, Krueger-Hadfield SA (2021) Package "poppr", Genetic Analysis of Populations with Mixed Reproduction

Kassambara A (2021) Package 'rstatix'', Pipe-Friendly Framework for Basic Statistical Tests'

Kenkel CD, Goodbody-Gringley G, Caillaud D, Davies SW, Bartels E, Matz MV (2013) Evidence for a host role in thermotolerance divergence between populations of the mustard hill coral (*Porites astreoides*) from different reef environments. Mol Ecol 22:4335–4348

Kopelman NM, Mayzel J, Jakobsson M, Rosenberg NA, Mayrose I (2015) CLUMPAK: a program for identifying clustering modes and packaging population structure inferences across K. Mol Ecol Resour 15:1179–1191

Korneliussen TS, Albrechtsen A, Nielsen R (2014) ANGSD: analysis of next generation sequencing data. BMC Bioinform 15:1–13

Korneliussen TS, Moltke I (2015) NgsRelate: a software tool for estimating pairwise relatedness from next-generation sequencing data. Bioinformatics 31:4009–4011

Kuffner IB, Toth LT (2016) A geological perspective on the degradation and conservation of western Atlantic coral reefs. Conserv Biol 30:706–715

Langmead B, Salzberg SL (2012) Fast gapped-read alignment with Bowtie 2. Nat Methods 9:357–359

Lee TN, Mayer DA (1977) Low-frequency current variability and spin-off eddies along the shelf off Southeast Florida. J Mar Res 35:193–220

Lenz EA, Bartlett LA, Stathakopoulos A, Kuffner IB (2021) Physiological differences in bleaching response of the coral *Porites astreoides* along the Florida keys reef tract during high-temperature stress. Front Mar Sci 8:1–14

Li Y-L, Liu J-X (2018) StructureSelector: a web-based software to select and visualize the optimal number of clusters using multiple methods. Mol Ecol Resour 18:176–177

Liu H, Stephens TG, González-Pech RA, Beltran VH, Lapeyre B, Bongaerts P, Cooke I, Aranda M, Bourne DG, Forêt S, Miller DJ, van Oppen MJH, Voolstra CR, Ragan MA, Chan CX (2018) Symbiodinium genomes reveal adaptive evolution of functions related to coral-dinoflagellate symbiosis. Commun Biol 1:1–11

López-Legentil S, Pawlik JR (2009) Genetic structure of the Caribbean giant barrel sponge *Xestospongia muta* using the I3–M11 partition of COI. Coral Reefs 28:157–165

Lord KS, Lesneski KC, Buston PM, Davies SW, D'Aloia CC, Finnerty JR (2023) Rampant asexual reproduction and limited dispersal in a mangrove population of the coral *Porites divaricata*. Proc R Soc B Biol Sci 290:1–11

Manzello DP, Matz MV, Enochs IC, Valentino L, Carlton RD, Kolodziej G, Serrano X, Towle EK, Jankulak M (2019) Role of host genetics and heat-tolerant algal symbionts in sustaining populations of the endangered coral *Orbicella faveolata* in the Florida Keys with ocean warming. Glob Chang Biol 25:1016–1031

Martin M (2011) Cutadapt removes adapter sequences from high-throughput sequencing reads. Embnet.journal 17:1–3

McDermond J, Brown S, Burt JA, Smith EG, Warren C, Dupont J, A AAM, McDermond J, Mangubhai S (2014) Reproduction and Population of *Porites divaricata* at Rodriguez Key: The Florida Keys, USA. Nova Southeastern University

Meirmans PG (2014) Nonconvergence in Bayesian estimation of migration rates. Mol Ecol Resour 14:726–733

Mussmann SM, Douglas MR, Chafin TK, Douglas ME (2019) BA3-SNPs: Contemporary migration reconfigured in BayesAss for next-generation sequence data. Methods Ecol Evol 10:1808–1813

Nazareno AG, Bemmels JB, Dick CW, Lohmann LG (2017) Minimum sample sizes for population genomics: an empirical study from an Amazonian plant species. Mol Ecol Resour 17:1136–1147

Neves EG, Andrade SCS, Da Silveira FL, Solferini VN (2008) Genetic variation and population structuring in two brooding coral species (*Siderastrea stellata* and *Siderastrea radians*) from Brazil. Genetica 132:243–254

NOAA (2018) Stony Coral Tissue Loss Disease Case Definition. Florida Keys Natl Mar Sanctuary

Oksanen J, Blanchet FG, Friendly M, Kindt R, Legendre P, Mcglinn D, Minchin PR, Hara RBO, Simpson GL, Solymos P, Stevens MHH, Szoecs E, Wagner H (2020) Package "vegan." 2395–2396

Pembleton LW (2021) Package "StAMPP", Statistical Analysis of Mixed Ploidy Populations

Perry CT, Steneck RS, Murphy GN, Kench PS, Edinger EN, Smithers SG, Mumby PJ (2015) Regional-scale dominance of non-framework building corals on Caribbean reefs affects carbonate production and future reef growth. Glob Chang Biol 21:1153–1164

Precht WF, Gintert BE, Robbart ML, Fura R, van Woesik R (2016) Unprecedented disease-related coral mortality in Southeastern Florida. Sci Rep 6:1–11

Puechmaille SJ (2016) The program STRUCTURE does not reliably recover the correct population structure when sampling is uneven: subsampling and new estimators alleviate the problem. Mol Ecol Resour 16:608–627

Rambaut A, Drummond AJ, Xie D, Baele G, Suchard MA (2018) Posterior summarization in Bayesian phylogenetics using Tracer 1.7. Syst Biol 67:901–904

Rippe JP, Dixon G, Fuller ZL, Liao Y, Matz M (2021) Environmental specialization and cryptic genetic divergence in two massive coral species from the Florida Keys Reef Tract. Mol Ecol 30:3468–3484

Riquet F, Japaud A, Nunes FLD, Serrano XM, Baker AC, Bezault E, Bouchon C, Fauvelot C (2021) Complex spatial patterns of genetic differentiation in the Caribbean mustard hill coral *Porites astreoides*. Coral Reefs 41:813–828

Ruiz-Moreno D, Willis BL, Page AC, Weil E, Cróquer A, Vargas-Angel B, Jordan-Garza AG, Jordán-Dahlgren E, Raymundo L, Harvell CD (2012) Global coral disease prevalence associated with sea temperature anomalies and local factors. Dis Aquat Organ 100:249–261

Serrano XM, Baums IB, Smith TB, Jones RJ, Shearer TL, Baker AC (2016) Long distance dispersal and vertical gene flow in the Caribbean brooding coral *Porites astreoides*. Sci Rep 6:1–12

Shay LK, Cook TM, Peters H, Mariano AJ, Weisberg R, An PE, Soloviev A, Luther M (2002) Very high-frequency radar mapping of surface currents. IEEE J Ocean Eng 27:155–169

Shoguchi E, Beedessee G, Hisata K, Tada I, Narisoko H, Satoh N, Kawachi M, Shinzato C (2021) A new dinoflagellate genome illuminates a conserved gene cluster involved in sunscreen biosynthesis. Genome Biol Evol 13:1–7

Shoguchi E, Shinzato C, Kawashima T, Gyoja F, Mungpakdee S, Koyanagi R, Takeuchi T, Hisata K, Tanaka M, Fujiwara M, Hamada M, Seidi A, Fujie M, Usami T, Goto H, Yamasaki S, Arakaki N, Suzuki Y, Sugano S, Toyoda A, Kuroki Y, Fujiyama A, Medina M, Coffroth MA, Bhattacharya D, Satoh N (2013) Draft assembly of the *Symbiodinium minutum* nuclear genome reveals dinoflagellate gene structure. Curr Biol 23:1399–1408

Skotte L, Korneliussen TS, Albrechtsen A (2013) Estimating individual admixture proportions from next generation sequencing data. Genetics 195:693–702

Snow G (2020) Package ' TeachingDemos ': Demonstrations for Teaching and Learning

Soloviev A, Luther ME, Weisberg RH (2003) Energetic baroclinic super-tidal oscillations on the Southeast Florida shelf. Geophys Res Lett 30:1–4

Soloviev AV, Hirons A, Maingot C, Dean CW, Dodge RE, Yankovsky AE, Wood J, Weisberg RH, Luther ME, McCreary JP (2017) Southward flow on the western flank of the Florida Current. Deep Res Part I Oceanogr Res Pap 125:94–105

Soong K (1991) Sexual reproductive patterns of shallow-water reef corals in Panama. Bull Mar Sci 49:832–846

Sturm AB, Eckert RJ, Méndez JG, González-Díaz P, Voss JD (2020) Population genetic structure of the great star coral, *Montastraea cavernosa*, across the Cuban archipelago with comparisons between microsatellite and SNP markers. Sci Rep 10:1–16

Sutherland K, Porter J, Torres C (2004) Disease and immunity in Caribbean and Indo-Pacific zooxanthellate corals. Mar Ecol Prog Ser 266:273–302

Szmant AM (1986) Reproductive ecology of Caribbean reef corals. Coral Reefs 5:43–53

Thornhill DJ, Fitt WK, Schmidt GW (2006) Highly stable symbioses among western Atlantic brooding corals. Coral Reefs 25:515–519

Toth LT, Stathakopoulos A, Kuffner IB, Ruzicka RR, Colella MA, Shinn EA (2019) The unprecedented loss of Florida's reef-building corals and the emergence of a novel coral-reef assemblage. Ecology 100:1–14

Tracy AM, Pielmeier ML, Yoshioka RM, Heron SF, Harvell CD (2019) Increases and decreases in marine disease reports in an era of global change. Proc R Soc B Biol Sci 286:20191718

Tyberghein L, Verbruggen H, Pauly K, Troupin C, Mineur F, De Clerck O (2012) Bio-ORACLE: a global environmental dataset for marine species distribution modelling. Glob Ecol Biogeogr 21:272–281

Vasquez Kuntz KL, Kitchen SA, Conn TL, Vohsen SA, Chan AN, Vermeij MJA, Page C, Marhaver KL, Baums IB (2022) Inheritance of somatic mutations by animal offspring. Sci Adv 8:1–11

Vega Thurber RL, Burkepile DE, Fuchs C, Shantz AA, Mcminds R, Zaneveld JR (2014) Chronic nutrient enrichment increases prevalence and severity of coral disease and bleaching. Glob Chang Biol 20:544–554

Vollmer AA (2018) Rare parthenogenic reproduction in a common reef coral. Nova Southeastern University, Porites astreoides

Walton CJ, Hayes NK, Gilliam DS (2018) Impacts of a regional, multi-year, multi-species coral disease outbreak in Southeast Florida. Front Mar Sci 5:1–14

Wang S, Meyer E, Mckay JK, Matz MV (2012) 2b-RAD: a simple and flexible method for genome-wide genotyping. Nat Methods 9:808–810

Willing EM, Dreyer C, van Oosterhout C (2012) Estimates of genetic differentiation measured by Fst do not necessarily require large sample sizes when using many SNP markers. PLoS ONE 7:1–7

Wilson GA, Rannala B (2003) Bayesian inference of recent migration rates using multilocus genotypes. Genetics 163:1177–1191

Wong K, Putnam HM (2022) *Porites astreoides* genome. (2022) Past_Genome. osf.io/ed8xu